Synthesis and Pharmacokinetics of a Dihydropyridine Chemical Delivery System for the Antiimmunodeficiency Virus Agent Dideoxycytidine

Paul F. Torrence,*,† Jun-ei Kinjo,† Shahrzad Khamnei,† and Nigel H. Greig‡

Section on Biomedical Chemistry, Laboratory of Medicinal Chemistry, National Institute of Diabetes and Digestive and Kidney Diseases, and Laboratory of Neurosciences, National Institute on Aging, National Institutes of Health, Bethesda, Maryland 20892

Received July 28, 1992

In order to explore the possibility that a dihydropyridine/pyridinium redox chemical delivery system might enhance significantly the brain uptake of the anti-HIV agent dideoxycytidine (DDC), we prepared a DDC derivative which bore the 1,4-dihydro-1-methyl-3-pyridylcarbonyl moiety at both the cytidine exocyclic amino moiety and the sugar 5′-hydroxyl function; namely, 5′,4*N*-bis-[(1,4-dihydro-1-methyl-3-pyridinyl)carbonyl]-2′,3′-dideoxycytidine (2). In cell-free extracts of rat brain tissue, compound 2 was readily converted to free DDC by stepwise oxidation and hydrolysis of the dihydropyridyl groups. Time-dependent plasma and brain concentrations of DDC and 2 were determined following iv administration of 2 (49.3 mg/kg) to rats. Compound 2 could be detected in brain, reaching peak concentrations of 7.7 ± 2.9 nmol/g at 15 min. Low levels of DDC also were detected with a peak concentration of 1.4 ± 0.5 nmol/g at 240 min after injection. The brain/plasma concentration integral of compound 2 was 0.95 whereas that for DDC in brain as a ratio of combined DDC and compound 2 levels in plasma was 0.24. Despite this, brain concentrations remained low and not significantly different from those achieved following administration of DDC alone.

Human immunodeficiency virus (HIV)-induced central nervous system (CNS) dysfunction,[1,2] probably caused by infected monocyte/macrophage-mediated virus transfer into the brain,[3–5] has been a major target of a number of studies designed to explore strategies to increase the blood–brain barrier penetration of anti-HIV agents.[6–11] The nucleoside, 2′,3′-dideoxycytidine (DDC), is one of the most potent dideoxynucleoside analogues in vitro, but it is much less effective than is AZT at penetration of the CNS based on measurements of cerebrospinal fluid concentrations.[12–15]

In this investigation, we have evaluated the utility of a dihydropyridine chemical delivery system[16–21] to enhance the brain uptake of 2′,3′-dideoxycytidine. Specifically, we prepared a DDC derivative (HP_2DDC) which bore the 1,4-dihydro-1-methyl-3-pyridinylcarbonyl moiety at both the cytidine exocyclic amino group and the sugar 5′-hydroxyl function.

Results

Chemistry. Synthesis (Scheme I). In one potential approach to derivatizing DDC (1) with a dihydropyridine redox system, one could envision synthesis of a nicotinate ester which would then be quaternized with methyl iodide to yield the *N*-methylpyridinium derivative which in turn could be reduced to the desired dihydropyridine. This approach was not feasible with 2′,3′-dideoxycytidine (DDC, 1) since the cytosine ring also would be alkylated both at the ring N3 position as well as the exocyclic amino moiety.[22] As an alternate strategy which avoided the necessity of protection of the exocyclic amino moiety of the cytosine ring, nicotinic acid methiodide was coupled to DDC (1) to give the presumed disubstituted DDC trigonellate (P_2-DDC) (Scheme I). This O- and N-acylated intermediate

Scheme I. Synthetic Route for the Preparation of 1,4-Dihydro-1-methyl-3-pyridylcarbonyl Derivatives of DDC

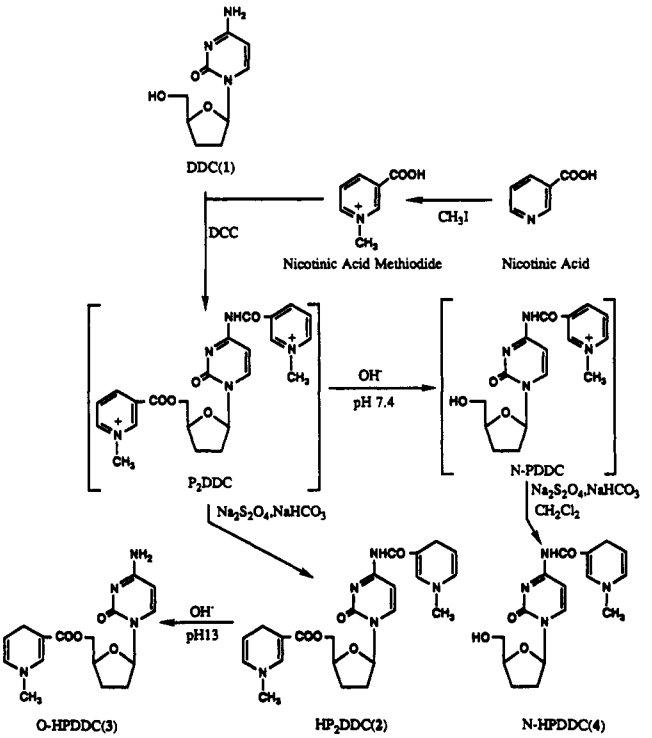

was not isolated but was further manipulated according to two different methodologies, depending upon the desired product. In the first approach, reduction of the diquaternized species with sodium dithionite gave the bis-dihydropyridinyl derivative (HP_2DDC, 2). Hydrolysis accomplished by overnight exposure to 0.1 M KOH in MeOH at room temperature gave the 5′-trigonellate ester of DDC (O-HPDDC, 3). The surprising preferential cleavage of the amide bond under these conditions can be rationalized by consideration of the resonance-stabilized

* To whom correspondence should be addressed at: Bldg 8/Rm B2A02, National Institutes of Health, Bethesda, MD 20892; phone 301-496-2653; FAX 301-402-0589.
† National Institute of Diabetes and Digestive and Kidney Diseases.
‡ National Institute on Aging.

anion that would facilitate collapse of the tetrahedral intermediate of amide hydrolysis.

In the alternative treatment, the P_2DDC intermediate was subjected to mild slightly alkaline hydrolysis at 37 °C to yield the N-acylated DDC derivative. This hydrolytic intermediate was not isolated as such, but was further treated with sodium dithionite to give N-HPDDC (4). The facile and preferential hydrolysis of the ester bond of the diquaternized intermediate, P_2DDC, under these conditions (vide infra), would be expected considering the considerable additional lability introduced to the ester bond by the proximal positively charged pyridinium group.

Chemical ionization mass spectroscopy provided a clear differentiation of the two monoacylated DDC derivatives. O-HPDDC (3) (M + H = 333) underwent essentially only one fragmentation to yield a peak at m/z = 222 corresponding to cleavage of the glycosidic linkage and the generation of a fragment ion consisting of the acylated sugar. This fragmentation pattern to give an ion from the acylated sugar was also witnessed in the CI-MS of N_2DDC as well as a dibenzoylated DDC (data not shown). N-HPDDC (4) (M + H = 333) showed predominant fragmentation with loss of the *N*-acyl moiety to give a peak m/z = 212, but significant fragmentation also occurred corresponding to loss of the sugar to give m/z = 233. Thus as with other nucleosides, there is a strong tendency for glycosidic bond cleavage, but in these particular materials, the charge partitions to the moiety bearing the dihydropyridyl group. In the case of the CI-MS of the disubstituted HP_2DDC (2) (M + H = 454), both modes of fragmentation were operative to produce peaks at m/z = 222 (acylated sugar) and 233 (acylated base).

The UV spectra of the synthetic derivatives also provided evidence for the assigned structures. The UV spectrum of O-HPDDC (3) (λ_{max} = 360 nm; ϵ = 6400; λ_{max} = 272 nm, ϵ = 11400) strongly resembled the UV spectrum of the previously reported[6] AZT derivative HPAZT [5′-[(1,4-dihydro-1-methyl-3-pyridinyl)carbonyl]-3′-azido-3′-deoxythymidine] (λ_{max} = 360 nm, ϵ = 7250; λ_{max} = 265 nm, ϵ = 13200). The other monosubstituted isomer, N-HPDDC (4), showed quite different behavior with λ_{max} = 388 nm (ϵ = 13000), λ_{max} = 297 nm (ϵ = 7100), and λ_{max} = 253 nm (ϵ = 12300). The disubstituted derivative of DDC, HP_2-DDC (2), displayed a UV spectrum that was a combination of the features of the two monosubstituted isomers with λ_{max} = 373 nm (ϵ = 11800), λ_{max} = 301 nm (ϵ = 9100), and λ_{max} = 254 nm (ϵ = 13700).

The disubstituted dihydropyridinyl DDC derivative 2 could be prepared in the amounts required for pharmacokinetic studies; however, the other monosubstituted derivatives (O-HPDDC and N-HPDDC) were considerably more difficult to access. Consequently, this study was concerned only with the brain/periphery partitioning of compound 2, HP_2DDC.

To provide an appropriate comparison of the redox prodrug HP_2DDC to another prodrug form of comparable lipophilicity but incapable of undergoing the essential redox conversion of the Bodor scheme, the disubstituted DDC derivative bis-nicotinoyl DDC (5, N_2DDC) also was prepared by a procedure analogous to that used for the synthesis of P_2DDC (scheme not shown).

Chemical Oxidation and Hydrolysis Studies. To gain some idea of the ease and course of oxidation and hydrolysis of the above DDC derivatives, oxidation by DDQ (2,3-dichloro-5,6-dicyano-1,4-benzoquinone) was examined. In addition, the stabilities of O-HPDDC (3) and N-HPDDC (4) in Tris–acetate buffer (pH 7.4, 37 °C) were evaluated (Figure 1).

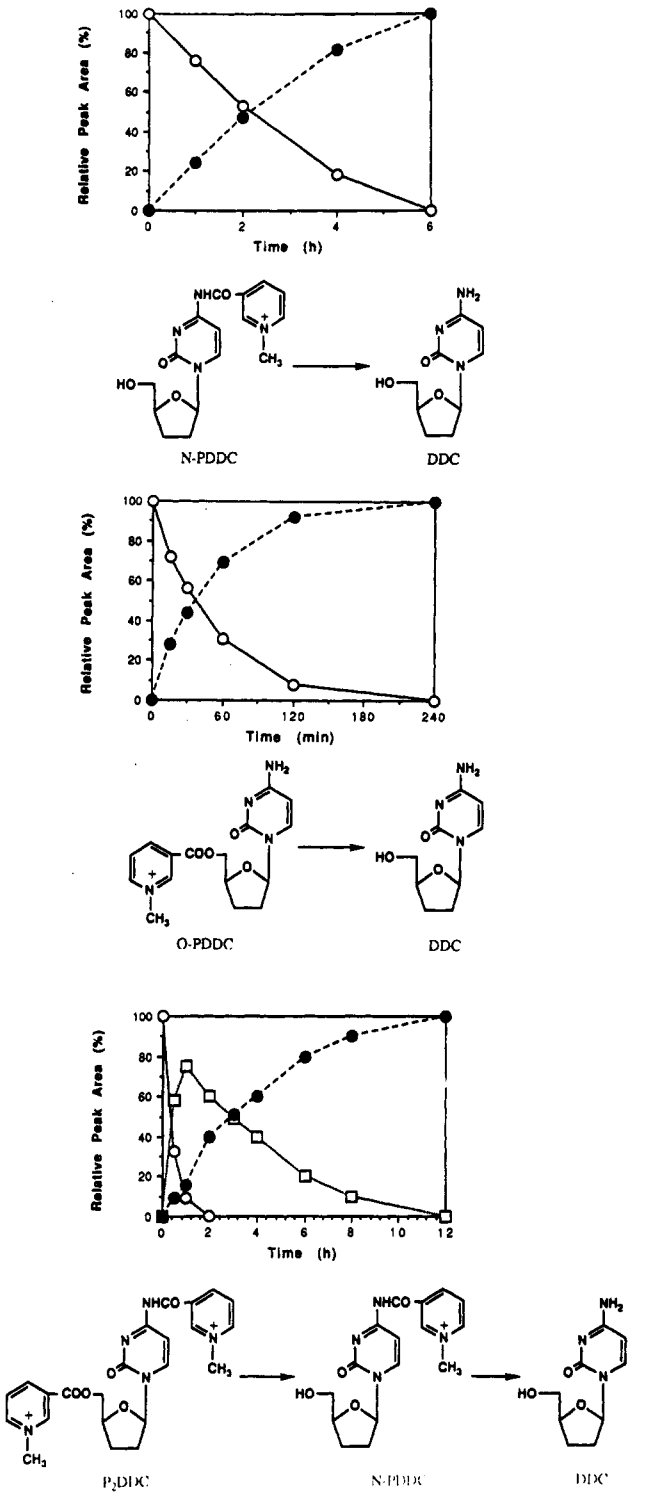

Figure 1. Hydrolytic behaviors of oxidized forms of HP_2DDC (2), O-HPDDC (3), and N-HPDDC (4). Top panel: hydrolysis of N-PDDC (○) to DDC (●); middle panel: hydrolysis of O-PDDC (○) to DDC (●); bottom panel: hydrolysis of P_2DDC (○) to N-PDDC (□) and finally DDC (●). The ordinate is the relative peak area as determined by integration of the appropriate peak from HPLC.

Generation of the requisite pyridinium derivatives was accomplished by shaking the precursors, N-HPDDC (4), O-HPDDC (3), and HP_2DDC (2) with DDQ in acetonitrile followed by treatment with DEAE-Sephadex to remove the resulting red pigment. Hydrolyses of the resulting

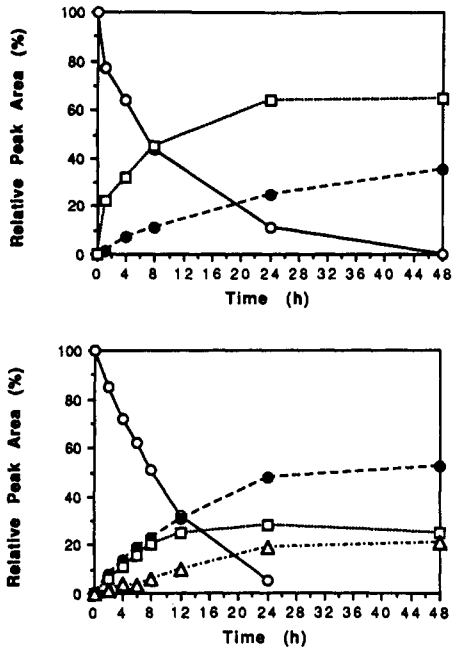

Figure 2. Top panel: decomposition of O-HPDDC (3) (○) in Tris buffer (pH 7.4) at 37 °C to give DDC (●) and an unidentified byproduct (□). Bottom panel: decomposition of HP_2DDC (4) (○) in Tris buffer (pH 7.4) at 37 °C to yield DDC (●) and two unidentified byproducts (□, △).

pyridinium salts were allowed to proceed in 50 mM Tris buffer (pH 7.4) at 37 °C, and aliquots were removed at various times for HPLC analysis. As recorded in Figure 1 (top), O-PDDC (2) was hydrolyzed to DDC (1) with 50% of the DDC being formed in 30 min. N-PDDC (4) also gave rise to DDC; however in this case, it required about 2 h for 50% of the resultant DDC to be produced (Figure 1, middle panel). The derivative which took the greatest amount of time (3 h) to produce DDC was P_2DDC (Figure 1, bottom). While the hydrolyses of the O-PDDC (3) and N-PDDC (4) were quite straightforward, the hydrolysis of P_2DDC was more complicated. There was a rapid disappearance of N_2DDC itself and the intermediate formation of N-PDDC which then hydrolyzed to DDC (Figure 1, bottom). The greater lability of the 5′-trigonellate ester bond in this situation mirrored its behavior during the synthesis of N-HPDDC (vide supra).

When either O-HPDDC (3) or N-HPDDC (4) was dissolved in Tris–acetate buffer (pH 7.4, 50 mM) containing 2% acetonitrile at a concentration of 2×10^{-4} M and maintained at 37 °C, extensive decomposition occurred as monitored by HPLC (Figure 2). In the case of O-HPDDC (3), the half-life for disappearance was approximately 7 h, but DDC (1) itself accounted for only about 30% of the product (Figure 2, top). The remaining material consisted of an unidentified byproduct. The half-life for decomposition of N-HPDDC (4) was about 9 h. In this instance, about 50% of the product consisted of DDC with the remaining material being roughly equal amounts of two unidentified byproducts (Figure 2, bottom). It is significant that in neither situation was any *O*- or *N*-pyridinium salt detected in contrast to the oxidation studies alluded to above. When HP_2DDC (2) was dissolved in the above buffer and its decomposition was followed under the same conditions, at least 15 products, including DDC (1) and N-HPDDC (4) could be detected (Figure 3).

Transformation of Dihydropyridyl Prodrugs by Rat Brain Cytosol. To determine whether or not HP_2-

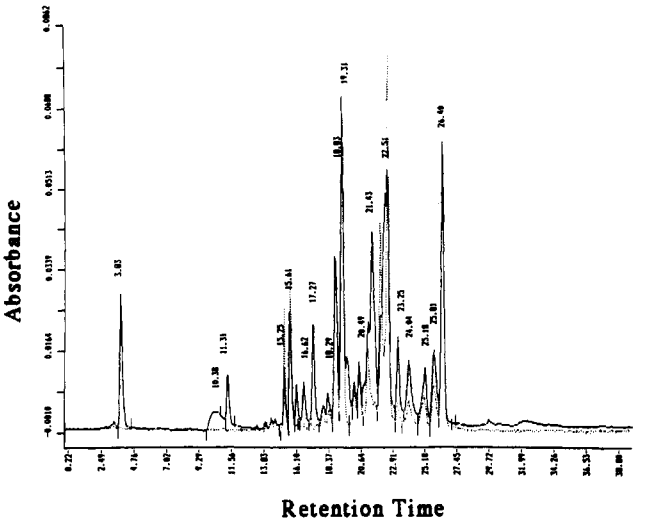

Figure 3. High performance liquid chromatogram of the decomposition of HP_2DDC (2) in Tris buffer pH 7.4, after 8 h incubation at 37 °C.

DDC (2), O-HPDDC (3), and N-HPDDC (4) could undergo the requisite series of reactions needed to fulfill their potential as prodrug forms which could be transported into the central nervous system and be oxidized to the positively charged pyridinium form, the metabolic fates of the above congeners were examined in cytoplasmic extracts of rat brain (Figure 4).

At 37 °C and pH 7.4, O-HPDDC (3) was converted gradually ($t_{1/2}$ approximately 2 h) to the pyridinium form, O-PDDC, which was subsequently hydrolyzed to DDC. Control incubations in the absence of extract provided, as in previous experiments (vide supra), only small quantities of DDC with no detectable pyridinium salt. The nitrogen-substituted analog N-HPDDC (4) behaved somewhat differently in that its $t_{1/2}$ (approximately 10 h) was considerably greater than the O-HPDDC. Also in contrast to its O-substituted isomer, N-HPDDC (4) gave rise to only low concentrations of the pyridinium form (N-PDDC), which in turn appeared to give rise to DDC. In the absence of rat brain cytosol, only minor amounts of DDC were formed.

Two conclusions could be drawn from the foregoing experiments. First, enzymic activities in the rat brain cytosol are needed to convert the dihydropyridyl prodrugs to their oxidized forms. These can then be hydrolyzed nonenzymatically to DDC as observed in the chemical oxidation experiments with DDQ. Secondly, the O-HPDDC derivative is more readily oxidized, and its pyridinium form, O-PDDC, is more readily hydrolyzed than N-HPDDC and its oxidized form N-PDDC. The more facile hydrolysis of O-PDDC as compared to N-PDDC would be expected from the ester versus amide nature of the linkages undergoing cleavage. It is not clear, however, why O-HPDDC should be more readily oxidized than N-HPDDC.

The disubstituted derivative, HP_2DDC (2), was transformed by rat brain cytosol in a manner completely predictable based on the results of the experiments with the monosubstituted analogues (Figure 5). HP_2DDC (2) itself quickly disappeared with a $t_{1/2}$ of approximately 30 min with a concurrent increase in concentration of the presumed O-P,N-HPDDC from which N-HPDDC was formed (Scheme II). This intermediate was then oxidized by the cytosolic enzymes to N-PDDC which then was

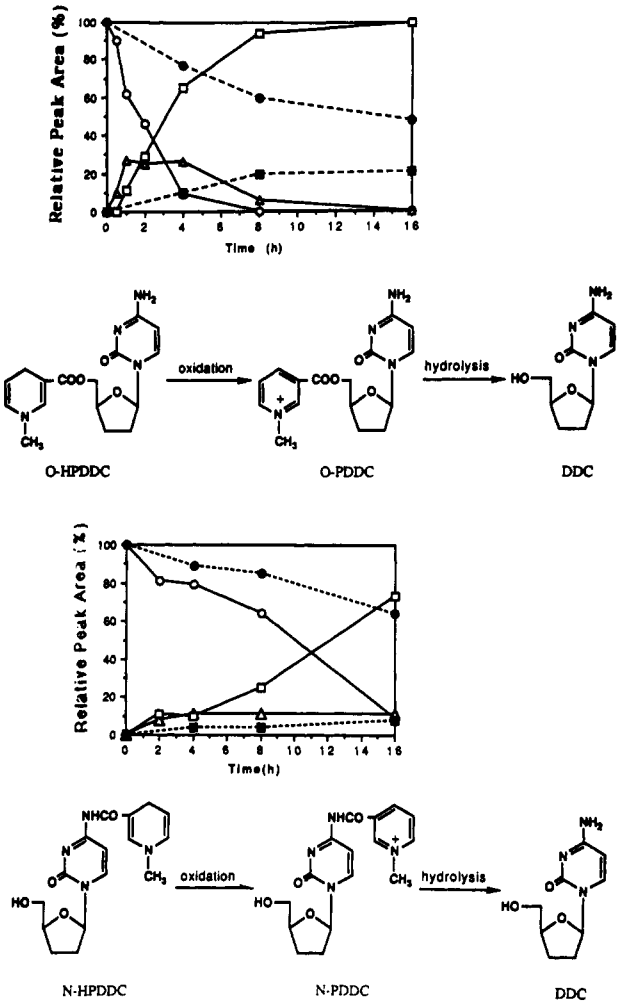

Figure 4. Metabolic transformations of O-HPDDC (3) and N-HPDDC (4) in the presence of rat brain cytosolic extract. Top panel: conversion of O-HPDDC (○) to O-PDDC (△) and DDC (□). In the absence of rat cytosol, there was a relatively slow decomposition of O-HPDDC (●), but little DDC (■) was formed. Bottom panel: transformations of N-HPDDC (○) to DDC (□) and N-PDDC (△). The decomposition of N-HPDDC under the same conditions but in the absence of rat brain extract (●) gave rise to little DDC (■).

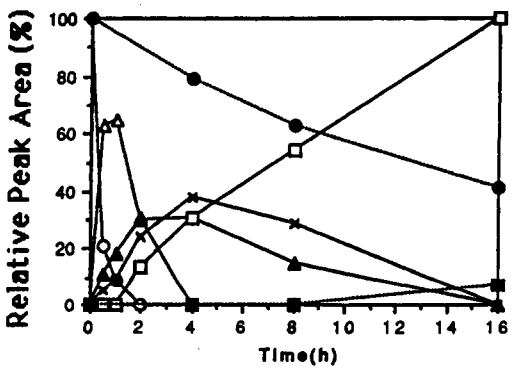

Figure 5. Metabolism of HP_2DDC (2) in the presence of rat brain cytosol: (○) HP_2DDC (2); (△) O-P, N-HPDDC; (▲) N-HPDDC; (×) N-PDDC; (□) DDC.

hydrolyzed to DDC. No evidence could be obtained from the HPLC of any formation of the disubstituted pyridinium form P_2DDC (Scheme II). The nonenzymatic formation of DDC was virtually insignificant under these conditions.

When evaluated for their ability to inhibit the growth of human immunodeficiency virus (HIV-1) in human lymphocyte MT-4 cells, O-HPDDC and N-HPDDC each gave IC_{50} values of 1.2×10^{-6} M, HP_2DDC showed an IC_{50} of 1.9×10^{-6} M, and DDC as reference standard had an IC_{50} of 1.0×10^{-6} M. These results suggested that all three dihydropyridyl derivatives could be transformed to DDC by cell cultures and were therefore virtually equivalent to DDC in their antiviral potential.

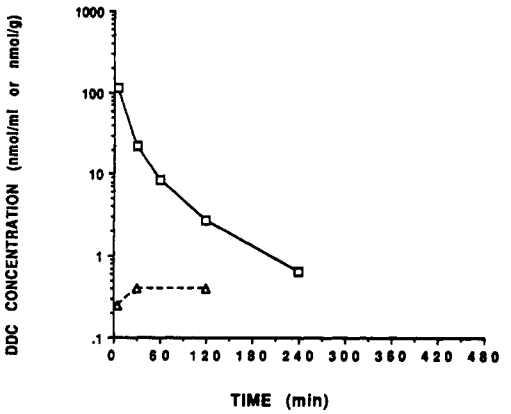

Figure 6. Plasma (□) and brain (△) DDC concentrations in rat after administration of 23 mg DDC/kg iv.

Table I. Pharmacokinetic Parameters

compound	plasma $t_{1/2}$, min	time-dependent concentration integral (nmol·min/mL) plasma	brain	ratio
DDC	22.7	3099 ± 256	126 ± 40	0.04
HP_2DDC	31.8	1510 ± 392	1444 ± 797	0.96
DDC (derived from HP_2DDC)		176 ± 88	408 ± 183	
N_2DDC	26.5	2139 ± 604	262 ± 113	0.12
DDC (derived from N_2DDC)	-	749 ± 131	109 ± 92	

Pharmacokinetics and Brain Uptake Studies. Figure 6 illustrates the time-dependent plasma and brain concentrations of DDC (1) following its iv administration to rats (23 mg/kg). A peak plasma level of 115.8 ± 3.3 nmol/mL occurred at 5 min, the earliest measured time, and thereafter DDC concentrations declined with a half-life of 22.7 min. No drug was detected after 240 min. Dramatically lower levels were present in brain, with a peak concentration of 0.44 ± 0.16 nmol/g occurring at 120 min. The *PA* of DDC (eq 4) was 3.4×10^{-6} s^{-1}, and its brain/plasma concentration integral ratio was 0.04 (Table I).

These results are in accord with those of Ibrahim and Boudinot[23] who have previously reported the rapid disappearance of DDC in rat following its iv administration. Renal clearance accounts for approximately 50% of DDC disappearance together with relatively low glucuronidation and biliary excretion and some 20% metabolism by the enzyme cytidine deaminase and anabolism to the pharmacologically active mono-, di-, and triphosphates. Our studies, additionally, are in accord with those of Kelly et al. who reported a CSF/plasma AUC ratio of 0.026 to 0.04 in rhesus monkeys.[13]

Figure 7 illustrates the time-dependent concentrations of HP_2DDC (2), DDC (1), and combined (total) levels in plasma and brain, respectively, following iv administration of HP_2DDC (49.3 mg/kg). A peak level of 36.6 ± 7.3 nmol/mL HP_2DDC (2) was detected in plasma at 5 min, which declined to 0.3 ± 0.1 nmol/mL at 480 min. Low concentrations of DDC were detected up to 240 min, with a peak

Scheme II. Metabolic Pathway of HP_2DDC in Rat Brain Cytosol

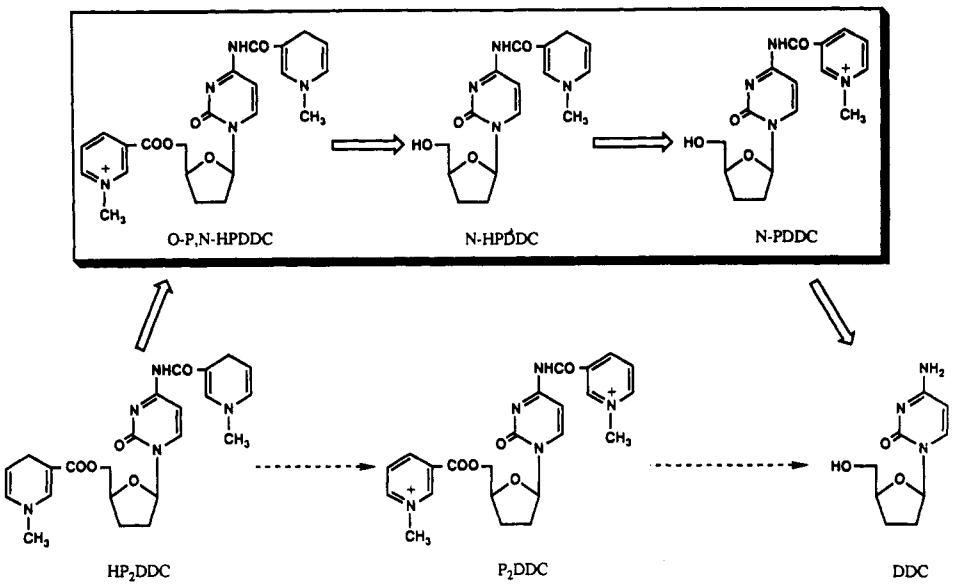

level of 2.0 ± 0.6 nmol/mL occurring at 5 min. HP_2DDC was detected in brain throughout the study, reaching a peak concentration of 7.7 ± 2.9 nmol/g at 15 min. It possessed a brain/plasma concentration integral of 0.95 (Table I). Despite this, only low levels of DDC were detected, with a peak concentration of 1.4 ± 0.5 nmol/g at 240 min. The low levels of DDC in brain were not dramatically different from those achieved following administration of DDC alone. Despite attempts to minimize HP_2DDC conversion to DDC in tissue samples during the analytical procedure, some conversion was bound to occur due to the inherent instability of HP_2DDC. Consequently, reported DDC concentrations could represent an overestimation.

Figure 8 illustrates the time-dependent concentrations of N_2DDC (5), DDC, and combined (total) levels in plasma and brain, respectively, after iv administration of N_2DDC (46 mg/kg). A peak concentration of 54.0 ± 2.1 nmol/mL N_2DDC (5) was detected in plasma at 5 min, declining to 1.9 ± 1.0 nmol/mL at 480 min. DDC was present in plasma between 5 and 120 min, with a peak level of 13.1 ± 2.2 nmol/mL at 5 min. Low concentrations of both N_2DDC (5) and DDC (1) were detected in brain throughout the study, with peak levels of 1.2 ± 0.4 nmol/g at 30 min and of 0.9 ± 0.7 nmol/g at 5 min, respectively. The brain/plasma concentration integral ratio of N_2DDC was 0.12. Likewise, brain levels of DDC were not dramatically different from those achieved following DDC or HP_2DDC administration. Figure 9 illustrates the comparative time-dependent concentration of DDC (1), HP_2DDC (2), and N_2DDC (5) in plasma following the equimolar iv administration of these compounds (Figure 9, left panel) and the concentration of DDC in brain, derived from these agents (Figure 9, right panel). Calculated pharmacokinetic parameters are shown in Table I. As illustrated in Figure 9 (left panel), the disappearance of DDC, HP_2DDC, and N_2DDC from plasma were similar, although a higher peak concentration was achieved after DDC injection. Furthermore, brain concentrations of DDC were low compared to total drug in plasma for each agent. Although HP_2DDC maintained the highest concentration in brain and achieved the largest time-dependent concentration integral, these were not significantly different from those achieved following equimolar administration of DDC or N_2DDC.

Discussion

Earlier studies[10,11] have concluded that, in the case of the application of the dihydropyridine–pyridinium redox chemical delivery system to the anti-HIV agent AZT, a

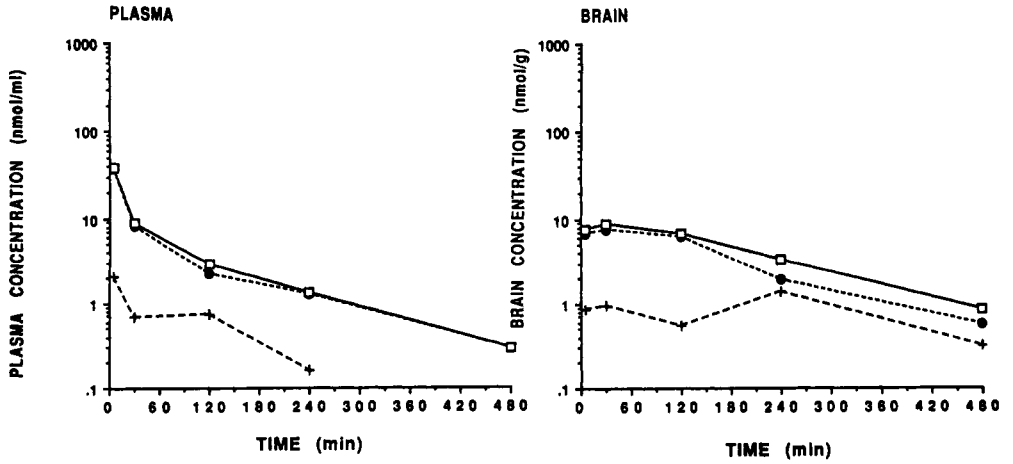

Figure 7. Plasma (left panel) and brain (right panel) total (□), HP_2DDC (●), and DDC (+) concentrations after administration of 49.3 mg/kg of HP_2DDC.

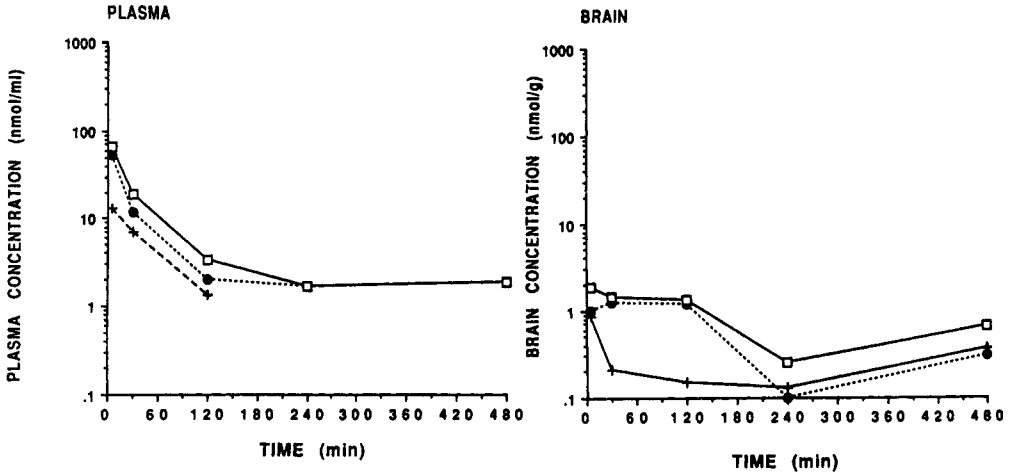

Figure 8. Plasma (left panel) and brain (right panel) total (□), N_2DDC (●) and DDC (+) concentrations after iv administration of 46 mg/kg of N_2DDC (5).

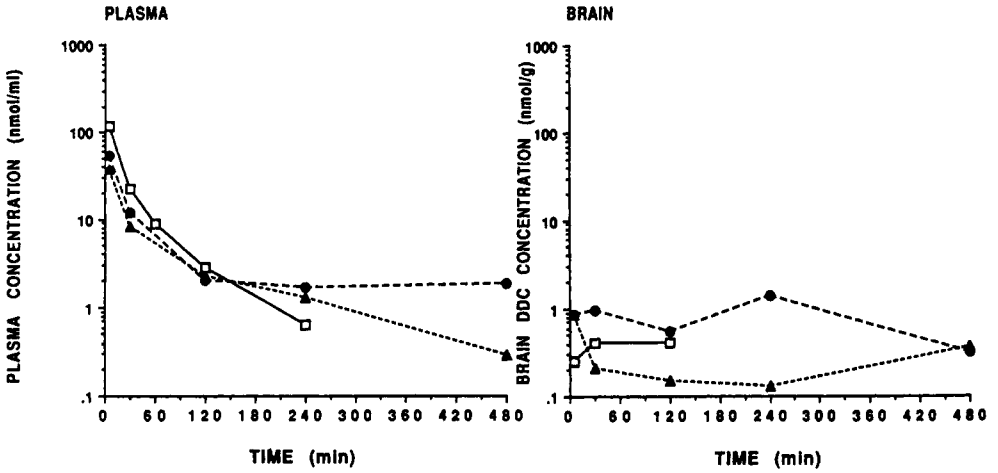

Figure 9. Left panel: DDC (1, □), HP_2DDC (2, ●), and N_2DDC (5, ▲) concentrations in plasma after administration of each, in separate experiments, in equimolar amounts. Right panel: DDC concentrations in brain after iv administration of equimolar quantities of DDC (□), N_2DDC (5, ▲), and HP_2DDC (2, ●).

significant increase in brain exposure to the antiviral agent was possible. In our attempts to apply this redox drug delivery system to DDC which is substantially less effective than is AZT at crossing the blood–brain barrier, we have not been able to demonstrate a significant increase in brain exposure to DDC after administration of the disubstituted redox prodrug, HP_2DDC (2), when compared either to DDC or to a lipophilic nonredox prodrug of DDC (5, N_2-DDC). We found that this dihydropyridyl derivative of DDC derivative relatively difficult to access synthetically as compared to the corresponding AZT derivative. The lipophilic nature of these materials represents a significant experimental difficulty which would surely complicate therapeutic application. For reasons we do not understand, the series of DDC derivatives (HP_2DDC, O-HPDDC, and N-HPDDC) were significantly less stable under mild conditions than was the corresponding AZT congener with which we have also worked. This instability also complicates experimental manipulation of these redox prodrug forms of DDC and, of course, would also be a therapeutic liability. It is possible that this lability may at least partly explain the failure of the application of this particular prodrug approach to achieving greater brain exposure to DDC.

These studies emphasize the importance of drug selection, AZT vs DDC, when attempting to utilize the dihydropyridine chemical delivery system to augment anti-AIDS drug delivery to the brain. Minor modifications in a drug may dramatically affect the ability of the redox prodrug form not only to reach the brain but also to release drug there via enzymatic action.[25] This could explain, in part, the highly variable results that others have found when attempting to use this chemical delivery system. Our attempts to employ this system for the anti-HIV agent DDC proved impractical for any possible clinical application where target concentrations of approximately 0.5 nmol/mL are required for inhibition of HIV replication.[26] Whereas such concentrations can be achieved in the plasma of patients,[27] it is unlikely that they could be achieved in brain without the administration of a severely toxic dose.

Experimental Section

Pharmacokinetics. Male Wistar rats, weighing approximately 120 g, were obtained from Charles Rivers Laboratories (Wilmington, MA). For iv drug administration, animals were anesthetized with halothane (Ayerst, New York, NY), the left saphenous vein was exposed, and an equimolar concentration (110 μmol/kg) of DDC (23 mg/kg), HP_2DDC (49.3 mg/kg), or N_2DDC (46 mg/kg), formulated in DMSO (2 mL/kg), was injected. From 5 to 480 min following drug administration, blood was collected by cardiac puncture, under halothane anesthesia, and the brain removed and placed on 0.9% NaCl, ice-chilled filter paper. Between three and eight animals were killed per time point. Blood was centrifuged (10000g, 30 s) and the plasma removed and frozen immediately to −70 °C. The left and right cerebral hemispheres were separated, frozen to −70 °C, and

weighed while frozen, and both brain and plasma samples then were analyzed for DDC, HP_2DDC, N_2DDC, and metabolites by HPLC.

Procedure for Analysis of Brain Samples. One brain hemisphere was homogenized in a Dounce homogenizer with an ice-cold mixture of DMSO (500–1000 μL) and 4 mL acetonitrile/water (3:1). Insoluble material and denatured protein were removed by centrifugation at 10000*g* for 10 min. The supernatant was removed, and solvent was removed in vacuo with the aid of a Speed-Vac (Savant). The residue was dissolved in DMSO/H_2O (1:1, 1.0 mL). This solution was applied to a column (8 × 30 mm) of DEAE-Sephadex ion-exchange resin. The effluent was collected, and the column was washed with an additional 2 mL of DMSO/H_2O (1:1). The washings and original effluent were combined and evaporated to dryness in a Speed-Vac. The residue was taken up in water and analyzed by HPLC under the conditions described below. The column employed was a Radial-Pak C18 reverse-phase cartridge (Waters). The HPLC system was Beckman system gold as described below. The analytical program was as follows: 1% solvent B in buffer A for 5 min with a flow rate of 2 mL/min; linear gradient for 40 min to 60% solvent B in buffer A. Buffer A was KH_2PO_4 10 mM, 5 mM PIC B (pH 6.9); solvent B was acetonitrile/water (9:1). Elution was monitored simultaneously at two wavelengths: 280 nm where DDC, N-HPDDC, O-HPDDC, N_2DDC, and HP_2DDC all absorbed; 380 nm where only the dihydropyridyl-substituted materials absorbed without interference from chromophores arising from cellular constituents. Isopropylidenecytidine was employed as a reference standard by spiking each sample before injection. Concentrations of DDC and its various derivatives were determined based on ratios between each unknown and the integrated area of the isopropylidenecytidine of known concentration. Recoveries were as follows: DDC, 50%; HP_2DDC, 55%; N-HPDDC, 37%; N_2-DDC, 60%.

Calculations. Concentrations of DDC, HP_2DDC, and N_2-DDC were calculated in brain samples from their net regional tissue concentrations, as measured with HPLC, by subtracting the intravascular volumes at the time of death (*T*). The intravascular concentration equaled the plasma concentration of the compound (nmol/mL) at time *T*, multiplied by the regional plasma volume (mL/g of tissue). Regional plasma volume was measured by injecting 3 anesthetized rats iv with [^{14}C]-methyl bovine serum albumin (17 μCi/mg, New England Nuclear Research Products, Boston, MA). This was determined to be 99.5% pure by polyacrylamide slab electrophoresis. Blood and brain samples were collected at 2 min, as described previously. [^{14}C]-Methyl bovine serum albumin, MW 69000 Da, remains within the cerebral vasculature during the 2-min experiment.

Regional blood volume was calculated by dividing the ^{14}C-activity of a brain sample by the ^{14}C-activity in blood (dpm·g^{-1}/dpm·mL) and equaled 1.7%. Concentration versus time data for DDC, HP_2DDC, and N_2DDC in plasma, between 5 and 120 min, were fitted by nonlinear regression analysis to a single exponential equation, where

$$C_{pl} = Ae^{-\alpha t} \quad (1)$$

In this equation, C_{pl} equals the concentration of compound (nmol/mL) at time *t* (min). A is defined as the theoretical zero time concentration in a central compartment, and α is the apparent first-order elimination rate constant (min). Plasma half-life was calculated from the parameters by the general formula:

$$t_{1/2} = 0.693/\alpha \quad (2)$$

Areas under the concentration–time profiles were calculated by the trapezoidal rule.

Finally, the cerbrovascular permeability of DDC was calculated at 30 min according to the two-compartmental model of Ohno et al.[28] This assumes no back-diffusion or loss of compound from brain. Whereas these assumptions probably are true for DDC, they are not for HP_2DDC and N_2DDC, due to their metabolism in brain and potential back-diffusion as a consequence of their lipophilicity. Therefore the cerebrovascular permeability of HP_2-DDC and N_2DDC were not calculated.

The unidirectional brain uptake of DDC is defined as

$$\Delta C_{br}/\Delta t = PA \cdot C_{pl} \quad (3)$$

where *PA* (s^{-1}) is cerebrovascular permeability (*P*; cm/s) × capillary surface area (*A*; cm^2/g brain, or cm^2/cm^3 brain), and C_{br} (nmol/g) is the brain parenchymal concentration, with the intravascular space subtracted. Eq 3 can be integrated to the time of death, *T* (30 min), to give the *PA* in terms of the arterial plasma concentration integral, eq 4.

$$PA = C_{br}(T)/C_{pl} \cdot \Delta t \quad (4)$$

Statistical Analysis. A two-tailed Student's *t*-test was performed for the comparison of two means. When more than two means were compared, one-way analysis of variance and a Bonferroni multiple *t*-test were utilized. Statistical significance for all tests was assessed at the 5% confidence level. Means ± SE are given routinely, unless otherwise noted.

Synthesis of 1,4-Dihydropyridinylcarbonyl Analogs of 2′,3′-Dideoxycytidine. Reagents. 2′,3′-Dideoxycytidine (DDC) was obtained from the National Cancer Institute (Bethesda, MD). *N*,*N*′-dicyclohexylcarbodiimide (DCC) and 1-hydroxybenzotriazole hydrate (HOBT) were purchased from Aldrich Chemical Co. (Milwaukee, WI). 2,3-Dichloro-5,6-dicyano-1,4-benzoquinone (DDQ) and sodium dithionite were obtained from Fluka Chemie AG (Switzerland). Sodium bicarbonate and sodium phosphate (dibasic) were from Allied Chemical (Morristown, NJ). PIC B-8 reagent (1-Octanesulfonic acid, sodium salt) was from Waters (Millipore Corp., Milford, MA).

TLC Analysis. Analytical TLC was on precoated Silica gel GHLF plates (250 μm, F254) from Analtech (Newark, DE). As solvent system, $CHCl_3$/MeOH (9:1) was used for DDC and its 1,4-dihydropyridinylcarbonyl derivatives: TLC R_f, DDC, 0.12; HP_2DDC, 0.80; O-HPDDC, 0.33; N-HPDDC, 0.57.

Centrifugally Accelerated TLC. The system employed the Chromatron (Model 7924T) from Harrison Research (Palo Alto, CA). The adsorbent was silica gel 60 PF-254, 1-mm layers. The solvent was CH_3CN/H_2O (9:1).

HPLC Analysis. The HPLC was System Gold from Beckman Instruments (Berkeley, CA). It consisted of two Model 110B Solvent Delivery Modules, an analog interface Module 406, and a Scanning Detector Module 167. The column was μ-Bondapak C18 reverse-phase (3.9 × 300 mm) (Waters-Millipore Corp., Milford, MA) with elution using the following conditions: solvent A, 10 mM sodium phosphate with 10 mM PIC B-8 reagent; solvent B, CH_3CN/H_2O (9:1); flow rate, 1.0 mL/min; 0.60% B (20 min), 60% B (15 min). The retention times were the following: DDC, 12.0 min; HP_2DDC, 26.2 min; O-HPDDC, 21.2 min; N-HPDDC, 19.5 min.

Spectral Measurements. Proton NMR spectra (300 MHz) were recorded on a Varian XL-300 spectrometer. The solvent was either DMSO-d_6 or $CDCl_3$ (TMS as an internal standard). Chemical shifts are reported in ppm. Multiplicity is abbreviated as s (singlet), d (doublet), t (triplet), and m (multiplet). Coupling constants are expressed in hertz (Hz). UV spectra were determined on a Beckman DU-8B spectrophotometer and mass spectra on a Finnigan/Extrel 1015 (chemical ionization instrument).

Nicotinic acid methiodide was prepared in a manner similar to that reported by Sarret et al.[23] for nicotinic acid chloride. Nicotinic acid (10.3 g, 8.4 mmol) was dissolved in MeOH (250 mL) under reflux. After addition of iodomethane (20 mL, 320 mmol), the solution was stirred for 12 h at 70 °C and then cooled. The resulting crude yellow crystals were collected by filtration. Recrystallization from a small amount of acetone gave nicotinic acid methiodide (17.8 g, 7.5 mmol, 80% yield); UV λ_{max} (MeOH) = 265 nm (ε = 3700), 218 (ε = 17700); ^{1}H-NMR (DMSO-d_6) δ 4.30 (s, 3, NCH_3), 8.0 (dd, 1, *J* = 8, 6 Hz, 5-H), 8.69 (d, 1, *J* = 8 Hz, 4 H), 8.75 (d, 1, *J* = 6 Hz, 6-H), 8.98 (s, 1, 2-H).

HP_2DDC [5′,4*N*-Bis[(1,4-dihydro-1-methyl-3-pyridinyl)-carbonyl]-2′,3′-dideoxycytidine] (2). DDC (211 mg, 1 mmol) and nicotinic acid methiodide (795 mg, 3 mmol) were suspended in pyridine. Dicyclohexylcarbodiimide (2.1 g, 1 mmol) and HOBT (1.35 g, 10 mmol) were added to this solution. Aliquots were removed and analyzed once a day. The reaction mixture was stirred for 3 d at ambient temperature. After evaporation of

pyridine in vacuo, H_2O was added to the residue and filtered. The filtrate was extracted with CH_2Cl_2 several times for removal of DCC and dicyclohexylurea. The aqueous layer was concentrated further and filtered to remove crystallized HOBT. After the solution was evaporated, the residue was dried in vacuo. This residue, which included dinicotinyl DDC dimethiodide [5′,4*N*-bis(1-methyl-3-pyridiniumcarbonyl)-2′,3′dideoxycytidine] (P_2DDC), was not subjected to further purification. The residue was dissolved into cold deaerated water (10 mL). $NaHCO_3$ (630 mg, 7.5 mmol) and $Na_2S_2O_4$ (870 mg, 5 mmol) were added to this solution, and the reaction mixture was stirred for 20 min at ambient temperature and then filtered. The precipitate (2, 164 mg, 37%) was crystallized from MeOH/H_2O: UV λ_{max} (MeOH) 373 (ϵ = 11800), 301 (ϵ = 9100), 254 (ϵ = 13700); CI-MS *m/z* 454 (M + H), 233, 222 (base); ^{1}H-NMR ($CDCl_3$) δ 1.8–2.6 (m, 4, 2′, sugar 2′- and 3-H's), 2.95, 2.99 (s, each 3, pyridine NMe's), 3.10, 3.20 (br s, each 2, 2 pyridine ring H's); 4.36 (m, 1, sugar 4′-H); 4.41 (br s, 2, sugar 5′-H's); 4.82 (m, 2, 2 pyridine 5-H's), 5.67 (m, 2, 2 pyridine 6-H's), 6.05 (m, 1, sugar 1′-H), 6.99, 7.07 (s, each 1, 2 pyridine 2-H's), 7.48 (d, 1, J = 7 Hz, cytosine 5-H), 8.12 (d, 1, J = 7 Hz, cytosine 6-H); HRMS (FAB) calcd for $C_{23}H_{31}N_5O_5$ (M^+) 453.2012, found 453.0007. Anal. ($C_{23}H_{31}N_5O_5 \cdot 2H_2O$) C, H; N: calcd for 14.30, found, 13.76.

O-HPDDC [5′-[(1,4-Dihydro-1-methyl-3-pyridinyl)carbonyl]-2′,3′-dideoxycytidine] (3). HP_2DDC (20 mg, 0.044 mmol) was dissolved in 0.1 M KOH/MeOH solution (1 mL). The mixture was kept overnight at room temperature and then applied to a column of silica gel (10 g). Elution was with $CHCl_3$/MeOH (19:1 then 9:1). After appropriate fractions were combined and evaporated, they were subjected to preparative, centrifugally accelerated, radial thin-layer chromatography (Chromatotron). A blue fluorescent band was collected to give O-HPDDC (3, 6.8 mg, 46%): UV λ_{max} (MeOH) 355 nm (ϵ = 7500), 278 nm (ϵ = 17800); CI-MS *m/z* 333 (M + H), 222 (base); ^{1}H-NMR ($CDCl_3$) δ 2.0–2.6 (m, 4, sugar 2′-, 3′-H's), 2.94 (s, 3, NCH_3), 3.10 (br s, 2, pyridine 4-H's), 4.36 (m, 3, sugar 4′,5′-H), 4.78 (dt, 1, J = 8, 4 Hz, pyridine 5-H); 5.66 (m, 2, cytosine 5-H and pyridine 6-H), 6.04 (dd, 1, J = 7, 3 Hz, sugar 1′-H), 6.99 (s, 1, pyridine 2-H), 7.79 (d, 1, J = 8 Hz, cytosine 6-H); HRMS (FAB) calcd for 333.1563 (M^+), found 333.1571. Anal. ($C_{16}H_{20}N_4O_4$) C, H, N.

N-HPDDC [4*N*-[(1,4-Dihydro-1-methyl-3-pyridinyl)carbonyl]-2′,3′-dideoxycytidine] (4). The fraction including dinicotinyl DDC dimethiodide (P_2DDC) was dissolved in H_2O and the resulting solution was adjusted to pH 7.5 with NaOH. The solution was incubated for 2 h at 37 °C and then cooled. $NaHCO_3$ (250 mg, 3 mmol), $Na_2S_2O_4$ (520 mg, 3 mmol) and CH_2Cl_2 were added to this solution. The biphasic mixture was stirred for 20 min at ambient temperature and the CH_2Cl_2 layer separated. The aqueous was additionally extracted with more CH_2Cl_2, and the combined CH_2Cl_2 extract was applied to a column of silica gel which was eluted with $CHCl_2$/MeOH (9:1). Appropriate fractions were combined to give after evaporation, N-HPDDC (4, 60 mg, 36%). Recrystallization from H_2O gave N-HPDDC (4) as fine yellow needles: UV λ_{max} = 338 (ϵ = 13000); 297 (ϵ = 7100), 253 (ϵ = 12300); CI-MS *m/z* 333 (M + H), 233; ^{1}H NMR ($CDCl_3$) δ 1.8–2.6 (m, 4, 2′-, 3′-H's), 2.92 (s, 3, NCH_3), 3.13 (s, 2, pyridine 4 H), 3.72 (dd, 1, J = 12, 4 Hz, 5′-H), 3.98 (dd, 1, J = 12, 2 Hz, 5′-H), 4.17 (m, 1, 4′-H), 4.78 (dt, 1, J = 8, 4 Hz, pyridine 5-H), 5.62 (dd, J = 8, 2 Hz, pyridine 6-H), 6.03 (dd, 1, J = 7, 3 Hz, 1′-H), 7.01 (s, 1, pyridine 2-H), 7.39 (d, 1, J = 7 Hz, 5-H), 8.21 (d, 1, J = 7 Hz, 6-H). HRMS (FAB) calcd for 333.1563 (M^+), found 333.1590. Anal. ($C_{16}H_{20}N_4O_4$) C, H, N.

N_2DDC [5′,4*N*-Bisnicotinyl-2′,3′-dideoxycytidine] (5). DDC (317 mg, 1.5 mmol) was suspended in pyridine (5 mL) and the resulting solution was warmed to 40 °C. Nicotinyl chloride (623 mg, 3.5 mmol) was added, and the homogeneous solution was stirred at 40 °C for 1 h. Additional nicotinyl chloride (356 mg, 2 mmol) was added, and this mixture was warmed overnight at 40 °C. Pyridine was removed by evaporation in vacuo. Water was added to the residue, and the resulting suspension was filtered. Silica gel chromatography [elution with $CHCl_3$/MeOH (19:1)] gave a residue, after evaporation of appropriate fractions, which was crystallized from MeOH to give 180 mg (43%) of N_2DDC (5): NMR ($CDCl_3$) δ 1.7–2.7 (m, 4, 2′,3′-H's), 4.55 (m, 1, 4′-H), 4.70 (m, 2, 5′-H's), 6.10 (m, 1, H-1′), 7.20 (br s, 1, N-H), 7.49 (m, 2, pyridine 5-H), 8.20 (d, J = 7 Hz, 1, cytosine 5-H), 7.38 (d, J = 7 Hz, 1, cytosine 6-H), 8.32 (m, 2, pyridine 4-H), 8.84 (m, 2, pyridine 6-H), 9.21 (s, 1, pyridine 2-H), 9.28 (s, 1, pyridine 2-H); MS (EI) *m/z* 421 (M^+), 217 (b + H); HRMS (FAB) calcd for $C_{21}H_{19}N_5O_5$ (M^+) 421.1386, found 421.1417.

Chemical Oxidation Studies. 1. Oxidation by DDQ and Subsequent Hydrolysis to DDC. DDQ (2 μmol in 40 μL CH_3CN) was added to 1 μmol of dihydropyridinyl derivative dissolved in 100 μL of CH_3CN. The mixture was shaken several times. In order to remove red pigment, DEAE Sephadex A-25 (360 μL, HCO_3^- form) was added to this mixture which was subsequently filtered. The filtrate was adjusted to 1.0 mL with Tris-AcOH buffer (50 mM, pH 7.4). The solution was maintained at 37 °C and aliquots were removed at various times for HPLC analysis.

2. Decomposition of Dihydronicotinyl Analogs. An amount of 1 μmol of dihydropyridinyl derivative (in 100 μL of CH_3CN) was diluted with Tris-AcOH buffer (50 mM, pH 7.4, 900 μL). This solution was kept at 37 °C. At various times, aliquots were removed and analyzed by HPLC using the same system as employed above.

Metabolism of Dihydropyridinyl Analogs. The three analogs separately were incubated at 37 °C in 10% DMSO/50 mM Tris, pH 7.4 with or without rat brain cytosol. At various time intervals (0, 0.5, 1, 2, 4, 8, and 16 h), aliquots were removed and diluted into 5 vols of ice-cold acetonitrile. These samples were kept at −80 °C until the conclusion of the reaction at which point all samples were centrifuged for 10 min at 1000*g*, and the supernatant was carefully removed from the precipitated protein. A 50-μL aliquot was evaporated by a stream of N_2 gas, and the residue was taken up in 100 μL of H_2O. Analysis was by HPLC using the elution program as described above. In the absence of brain extract, no pyridinium salt was formed under the same incubation conditions.

Acknowledgment. We are indebted to Drs. Jan Balzarini and Erik De Clercq who determined the HIV-1 inhibition potential of the compounds reported herein. This research was supported in part by the NIH Intramural Targeted Antiviral Program.

References

(1) Tucker, T. Central Nervous System AIDS. *J. Neurol. Sci.* **1989**, *89*, 119–132.
(2) Budka, H. Human Immunodeficiency Virus (HIV)-Induced Disease of the Central Nervous System: Pathology and Implications for Pathogenesis. *Acta Neuropathol.* **1989**, *77*, 225–236.
(3) Eilbott, D. J.; Peress, N.; Burger, H.; LaNeve, D.; Orenstein, J.; Gendelman, H.; Seidman, R.; Weiser, B. Human Immunodeficiency Virus Type 1 in Spinal Cords of Acquired Immunodeficiency Syndrome Patients with Myelopathy: Expression and Replication in Macrophages. *Proc. Natl. Acad. Sci. U.S.A.* **1989**, *86*, 3337–3341.
(4) Price, R. W.; Brew, B.; Sidtis, J.; Rosenblum, M.; Scheck, A. C.; Cleary, P. The Brain in AIDS: Central Nervous System HIV-1 Infection and AIDS Dementia Complex. *Science* **1988**, *239*, 586–592.
(5) Navia, B. A.; Jordan, B. D.; Price, R. W. The AIDS Dementia Complex: I Clinical Features. *Ann. Neurol.* **1986**, *19*, 517–524.
(6) Torrence, P. F.; Kinjo, J.; Lesiak, K.; Balzarini, J.; De Clercq, E. AIDS Dementia: Synthesis and Properties of a Derivative of 3′-Azido-3′-Deoxythymidine (AZT) that may become 'Locked' in the Central Nervous System. *FEBS Lett.* **1988**, *234*, 135–140.
(7) Palomino, E.; Kessel, D.; Horwitz, J. P. J. A Dihydropyridine Carrier System for Sustained Delivery of 2′,3′-Dideoxynucleosides to the Brain. *J. Med. Chem.* **1989**, *32*, 622–625.
(8) Chu, C. K.; Bhadti, V. S.; Doshi, K. J.; Etse, J. T.; Gallo, J. M.; Boudinot, F. D.; Schinazi, R. F. Brain Targeting of Anti-HIV Nucleosides: Synthesis and in Vitro and in Vivo Studies of Dihydropyridine Derivatives of 3′-Azido-2′,3′-Dideoxyuridine and 3′-Azido-3′-Deoxythymidine. *J. Med. Chem.* **1990**, *33*, 2188–2192.
(9) Gogu, S. R.; Aggarwal, S. K.; Rangan, S. R. S.; Agrawal, K. C. A Prodrug of Zidovudine with Enhanced Efficacy Against Human Immunodeficiency Virus. *Biochem. Biophys. Res. Comm.* **1989**, *160*, 656–661.
(10) Brewster, M. E.; Anderson, W.; Bodor, N. Brain, Blood, and Cerebrospinal Fluid Distribution of a Zidovudine Chemical Delivery System in Rabbits. *J. Pharm. Sci.* **1991**, *80*, 843–846.
(11) Aggarwal, S. K.; Gogu, S. R.; Rangan, S. R. S.; Agrawal, K. C. Synthesis and Biological Evaluation of Prodrugs of Zidovudine. *J. Med. Chem.* **1990**, *33*, 1505–1510.

(12) Klecker, R. W.; Collins, J. M.; Yarchoan, R. C.; Thomas, R.; McAtee, N.; Broder, S.; Myers, C. E. Pharmacokinetics of 2',3'-Dideoxycytidine in Patients with AIDS and Related Disorders. *J. Clin. Pharmacol.* **1988**, *28*, 837–842.
(13) Kelley, J. A.; Litterst, C. L.; Roth, J. S.; Vistica, D. T.; Poplack, D. G.; Conney, D. A.; Nadkarni, M.; Balis, F. M.; Broder, S.; Johns, D. G. The Disposition and Metabolism of 2',3'-Dideoxycytidine, An in Vitro Inhibitor of Human T-Lymphotrophic Virus Type III Infectivity, in Mice and Monkeys. *Drug Metab. Dispos.* **1987**, *15*, 595–601.
(14) Tomaszewski, J. E.; Grieshaber, C. K.; Balzarini, J.; Johns, D. G.; Smith, A. C.; Liao, J. T.; Collins, W. T., Jr. Toxicologic and Pharmacokinetic Evaluation of 2',3'Dideoxycytidine (ddCyd, NSC-606170), A Potential Drug to treat AIDS. *Proc. Am. Assoc. Cancer Res.* **1987**, *28*, 440.
(15) Collins, J. M.; Klecker, R. W.; Kelley, J. A.; Roth, J. S.; McCully, C. L.; Balis, F.; Poplack, D. G. Pyrimidine Dideoxyribonucleosides: Selectivity of Penetration into Cerebrospinal Fluid. *J. Pharmacol. Exp. Ther.* **1988**, *245*, 466–470.
(16) Bodor, N.; Brewster, M. E. Problems of Delivery of Drugs to the Brain. *Pharmacol. Ther.* **1983**, *19*, 337–396.
(17) Bodor, N. Targeting of Drugs to the Brain. *Methods Enzymol.* **1985**, *112*, 381–396.
(18) Bodor, N.; Nakamura, T.; Brewster, M. E. Improved Delivery Through Biological Membranes. Synthesis, Distribution, and Neurochemical Effects of a Tryptamine Chemical Delivery System. *Drug Des. Deliv.* **1986**, *1*, 51–64.
(19) Brewster, M. E.; Estes, K. S.; Bodor, N. Improved Delivery Through Biological Membranes. 32. Synthesis and Biological Activity of Brain-Targeted Delivery Systems for Various Estradiol Derivatives. *J. Med. Chem.* **1988**, *31*, 244–249.
(20) Wu, W.; Pop, E.; Shek, E.; Bodor, N. Brain-Specific Chemical Delivery Systems for β-Lactam Antibiotics. In Vitro and in Vivo Studies of Some Dihydropyridine and Dihydroisoquinoline Derivatives of Benzylpenicillin in Rats. *J. Med. Chem.* **1989**, *32*, 1782–1788.
(21) Pop, E.; Wu, W.; Shek, E.; Bodor, N. Brain-Specific Chemical Delivery Systems for β-Lactam Antibiotics. Synthesis and Properties of Some Dihydropyridine and Dihydroisoquinoline Derivatives of Benzypenicillin. *J. Med. Chem.* **1989**, *32*, 1774–1781.
(22) Sun, L.; Singer, B. Reaction of Cytidine with Ethylating Agent. *Biochemistry* **1974**, *13*, 1905–1913.
(23) Ibrahim, S. S.; Boudinot, F. D. Pharmacokinetics of 2',3'-Dideoxycytidine in Rats: Application to Interspecies. *J. Pharm. Pharmacol.* **1989**, *41*, 829–834.
(24) Sarret, H. P.; Perlzweig, W. A.; Levy, E. D. Synthesis and Excretion of Trigonelline. *J. Biol. Chem.* **1940**, *135*, 483–485.
(25) Buddy, A. V.; Zhang, K.; LePage, F.; Tombret, F.; Slatter, J. A.; Baillie, T. A.; Levy, R. H. In Vitro and in Vivo Investigation of Dihydropyridine-Based Chemical Delivery Systems for Anticonvulsants. *Pharm. Res.* **1991**, *8*, 690–697.
(26) Mitsuya, H.; Weinhold, J. K.; Furman, A. P.; Clair, ST. M.; Lehman, S.; Gallo, C. R.; Bolognesi, D.; Barry, W. D.; Broder, S. 3'-Azido-3'-Deoxythymidine (BW A509U): An Antiviral Agent that Inhibits the Infectivity and Cytopathic Effect of Human T-Lymphotropic Virus Type III/Lymphadenopathy-Associated Virus in Vitro. *Proc. Natl. Acad. Sci. U.S.A.* **1985**, *82*, 7096–7100.
(27) Yarchoan, R.; Perno, C. F.; Thomas, R. V.; Klecker, R. W.; Allain, J. P.; Wills, R. J.; McAtee, N.; Fischl, M. A.; Dubinsky, R.; McNeely, M. C.; Mitsuya, H.; Pluda, J. M.; Lawley, T. J.; Leuther, M.; Safai, B.; Collins, J. M.; Myers, C. E.; Broder, S. Phase I Studies of 2',3'-Dideoxycytidine in Sever Human Immunodeficiency Virus Infection as a Single Agent and Altering with Zidovudine (AZT). *Lancet* **1988**, *1*, 76–81.
(28) Ohno, K.; Pettigrew, K. D.; Rapaport, S. I. Lower Limits of Cerebrovascular Permeability to Nonelectrolytes in the Conscious Rat. *Am. J. Physiol.* **1979**, *235*, H299–H307.